LAWRENCE
LIVERMORE
NATIONAL
LABORATORY

LLNL-SM-655180

CoEVP: A Co-design Embedded ViscoPlasticity Scale-bridging Proxy App for ExMatEx

M. Dorr, N. Barton, J. Keasler, F. Li

June 2, 2014

Disclaimer

This work performed under the auspices of the U.S. Department of Energy by Lawrence Livermore National Laboratory under Contract DE-AC52-07NA27344.

CoEVP: A Co-design Embedded Viscoplasticity Scale-bridging Proxy App for ExMatEx

Milo Dorr, Nathan Barton, Jeffrey Keasler, Frankie Li

Last update: May 23, 2014

1 Introduction

The purpose of this document is to specify a proxy application named CoEVP (Co-design for Embedded ViscoPlasticity) being developed by the ExMatEx exascale computing co-design center [1]. CoEVP is intended to provide a greatly simplified implementation of a coarse "engineering" scale Lagrangian finite element model of a deforming material with an embedded viscoplasticity fine-scale model of constitutive properties. The approach closely follows that of [2, 3] in which viscoplasticity models were embedded in ALE3D [4] using an adaptive sampling approach. Due to the size and complexity of ALE3D, as well as restrictions on its distribution, we seek a substantial simplification of this earlier work in which the currently available LULESH proxy app [5] provides the coarse-scale model implementation and the ASPA proxy app [6] provides the adaptive sampling support. Arbitrary fine-scale viscoplasticity models can be added in a modular fashion, including synthetic responses based on abstract performance models if desired. This will better enable vendors and other researchers to investigate the exascale implications and requirements of scale-bridging applications implemented using a heterogeneous execution strategy.

2 Coarse-scale model

Lagrangian model

The macroscopic motion of the material system is described by a Lagrangian model of the evolution of position and velocity coordinates, $\mathbf{x}$ and $\mathbf{v}$,

$$\mathbf{x} \equiv \mathbf{x}(t), \qquad \mathbf{x}(0) = \mathbf{x}_0, \tag{1}$$

$$\mathbf{v} \equiv \dot{\mathbf{x}}(t), \qquad \mathbf{v}(0) = \mathbf{v}_0, \tag{2}$$

coupled with a momentum equation

$$\rho\dot{\mathbf{v}} = \nabla \cdot \boldsymbol{\sigma} + \rho\mathbf{f}, \tag{3}$$

where $\rho = \rho_0 \eta^{-1}$ is the density, ρ_0 is a reference density, η is the relative volume, $\boldsymbol{\sigma}$ is the Cauchy stress tensor and $\mathbf{f}$ is a body force density (*e.g.*, gravity). The specific internal energy e is evolved as

$$\rho_0 \dot{e} = \eta \boldsymbol{\sigma}' : \mathbf{D} - (p+q)\,\dot{\eta}. \tag{4}$$

Here, $q = q(\mathbf{v})$ is the bulk viscosity, and the deviatoric stress, strain rate, velocity gradient and pressure are given by

$$\boldsymbol{\sigma}' \equiv \boldsymbol{\sigma} + (p+q)\,\mathbf{I}, \tag{5}$$

$$\mathbf{D} \equiv \frac{1}{2}\left(\mathbf{L} + \mathbf{L}^T\right), \quad \mathbf{L} \equiv (\nabla \otimes \mathbf{v})^T, \tag{6}$$

$$p \equiv -\frac{1}{3}\mathrm{tr}(\boldsymbol{\sigma}) - q, \tag{7}$$

$$\boldsymbol{\sigma}' : \mathbf{D} \equiv \mathrm{tr}\left(\boldsymbol{\sigma}' \cdot \mathbf{D}^T\right) = \mathrm{tr}\left(\boldsymbol{\sigma}' \cdot \mathbf{D}\right), \tag{8}$$

respectively. To close the system, a constitutive model is required to specify $\boldsymbol{\sigma}$.

The system of equations (1)-(8) is the same as that solved by both ALE3D and LULESH, although, for simplification purposes in its role as a proxy app, the initial implementation of LULESH included only the volumetric stress component (*i.e.*, $\boldsymbol{\sigma}' = 0$), and the pressure was given by an ideal gas law $p = (\gamma - 1)\rho e$. The inclusion of material strength in CoEVP involves a full tensor $\boldsymbol{\sigma}$ and a different equation of state (described below).

Discretization

A finite element method is used to discretize (1)-(8). Letting Ω denote the spatial domain, a variational formulation of (3) is obtained by integrating it against a suitable space of test functions w, using integration by parts on the divergence term:

$$\int_\Omega \rho \dot{\mathbf{v}} w d\Omega + \int_\Omega \boldsymbol{\sigma} \cdot \nabla w d\Omega - \int_\Gamma \mathbf{n} \cdot \boldsymbol{\sigma} d\Gamma = \int_\Omega \rho \mathbf{f} w d\Omega, \qquad \forall w, \tag{9}$$

where $\Gamma \equiv \partial\Omega$ is the boundary of Ω and $\mathbf{n}$ is its outward-pointed unit normal. The spatial discretization results from limiting the position coordinate $\mathbf{x}$ (and therefore also $\mathbf{v}$) to a finite-dimensional subspace, as well as limiting the space of test functions to the same, or possibly different, finite-dimensional space. Numerical quadrature is then used to compute the integrals in the discrete variational form. Consequently, we require evaluations of $\boldsymbol{\sigma}$ at the corresponding quadrature points.

3 Strength model

Strain measure

Specification of the constitutive model yielding $\boldsymbol{\sigma}$ requires the introduction some measure of material strain together with a prescription for its evolution over a coarse-scale time step. As described in [2], the coarse-scale model couples to the fine-scale viscoplasticity model through a factorization of the material deformation gradient

$$\mathbf{F} = \mathbf{V} \cdot \mathbf{R} \cdot \mathbf{F}^p \tag{10}$$

into a symmetric, thermo-elastic stretch tensor $\mathbf{V}$, a rotation $\mathbf{R}$ between the fine- and coarse-scale reference frames, and a plastic deformation gradient $\mathbf{F}^p$. Since, by the chain rule,

$$\dot{\mathbf{F}} = \mathbf{L} \cdot \mathbf{F}, \tag{11}$$

the coarse-scale velocity gradient (6) may be evaluated using (10) as

$$\begin{aligned} \mathbf{L} &= \dot{\mathbf{F}} \cdot \mathbf{F}^{-1} \\ &= \dot{\mathbf{V}} \cdot \mathbf{V}^{-1} + \mathbf{V} \cdot \left(\dot{\mathbf{R}} \cdot \mathbf{R}^{\mathrm{T}} + \mathbf{R} \cdot \bar{\mathbf{L}} \cdot \mathbf{R}^{\mathrm{T}} \right) \cdot \mathbf{V}^{-1}, \end{aligned} \tag{12}$$

where the fine-scale velocity gradient is defined as

$$\bar{\mathbf{L}} = \dot{\mathbf{F}}^p \cdot (\mathbf{F}^p)^{-1}. \tag{13}$$

The kinematic system (12) therefore describes the evolution of $\mathbf{V}$ and $\mathbf{R}$ in terms of $\mathbf{L}$ and $\bar{\mathbf{L}}$. The integration of this system, which involves evaluations of the fine-scale plasticity model to obtain $\bar{\mathbf{L}}$, is described in Section 4. Using the resulting $\mathbf{V}$, we compute the logarithmic thermo-elastic strain measure

$$\mathbf{E} = \ln(\mathbf{V}). \tag{14}$$

Elasticity model

Letting

$$J = \det(\mathbf{V}), \quad a = J^{1/3}, \tag{15}$$

the volumetric component of $\bar{\mathbf{E}} = \mathbf{R}^{\mathrm{T}} \cdot \mathbf{E} \cdot \mathbf{R}$ (i.e., $\mathbf{E}$ in the fine-scale frame) is given by

$$\mathrm{tr}\left(\bar{\mathbf{E}}\right) = \ln\left(J\right), \tag{16}$$

and the deviatoric component approximated by

$$\bar{\mathbf{E}}' \approx \frac{1}{a} \bar{\mathbf{V}}'. \tag{17}$$

A simple elasticity model yielding the Cauchy stress $\boldsymbol{\sigma} = \mathbf{R} \cdot \bar{\boldsymbol{\sigma}} \cdot \mathbf{R}^{\mathrm{T}}$ needed by the coarse-scale model is

$$\bar{\boldsymbol{\sigma}} = -\left(p + q\right) \mathbf{I} + J^{-1} \bar{\boldsymbol{\tau}}' \tag{18}$$

where, assuming a constant shear modulus G, the deviatoric component of the Kirchoff stress $\boldsymbol{\tau} = J\boldsymbol{\sigma}$ is given by

$$\bar{\boldsymbol{\tau}}' = 2G\bar{\mathbf{E}}' = \frac{2G}{a} \bar{\mathbf{V}}'. \tag{19}$$

Equation of state and bulk viscosity

CoEVP provides two relatively similar equation of state options, although other models can be implemented by derivation from a C++ abstract base class defining a general interface to the rest of the code. In both models, we define the compression $\mu = \eta^{-1} - 1$.

Mie-Gruneisen: We consider the model presented in [7], where the pressure p is evaluated as

$$p = \left(k_1\mu + k_2\mu^2 + k_3\mu^3\right)\left(1 - \frac{\Gamma}{2}\mu\right) + \rho_0 e\Gamma\left(1+\mu\right). \tag{20}$$

Bulk Pressure: The pressure p is evaluated from the bulk pressure formula described in [8]:

$$p = p(\mu, e) \equiv p_g(\mu) + \rho_0 e\left(\Gamma_0 + \alpha\mu\right), \tag{21}$$

where

$$p_g(\mu) = \begin{cases} \dfrac{K_0\mu\left[1 + \left(1 - \frac{1}{2}\Gamma_0\right)\mu - \frac{1}{2}\alpha\mu^2\right]}{\left[1-\left(S-1\right)\mu\right]^2}, & \mu > 0. \\ K_0\mu, & \mu \leq 0, \end{cases} \tag{22}$$

The bulk viscosity q is of the same monotonically limited form [9] as currently implemented in LULESH, namely.

$$q = c_q\rho\left(a\nabla\cdot\mathbf{v}\right)^2 - c_\ell\rho c_s a|\nabla\cdot\mathbf{v}|, \tag{23}$$

where c_q and c_ℓ are parameters. The sound speed is estimated as

$$c_s = \left(K + \frac{4}{3}G\right)^{1/2}, \tag{24}$$

where K and G are the bulk and shear moduli, respectively.

4 Integration of the kinematic system

Reformulation

As described in [2], the integration of (12) is facilitated by a reformulation in terms of the symmetric and skew components of the fine- and coarse-scale velocity gradients (*i.e.*, strain rate and spin)

$$\mathbf{D} = \frac{1}{2}\left(\mathbf{L} + \mathbf{L}^{\mathrm{T}}\right), \quad \mathbf{W} = \frac{1}{2}\left(\mathbf{L} - \mathbf{L}^{\mathrm{T}}\right), \tag{25}$$

$$\bar{\mathbf{D}} = \frac{1}{2}\left(\bar{\mathbf{L}} + \bar{\mathbf{L}}^{\mathrm{T}}\right), \quad \bar{\mathbf{W}} = \frac{1}{2}\left(\bar{\mathbf{L}} - \bar{\mathbf{L}}^{\mathrm{T}}\right). \tag{26}$$

The system is simplified by assuming that the deviatoric component of $\mathbf{V}$ is small

$$\mathbf{V} = \frac{1}{a}\left(\mathbf{I} - \epsilon^*\right), \tag{27}$$

and that plasticity does not affect the material volume

$$\mathrm{tr}(\bar{\mathbf{L}}) = \mathrm{tr}(\bar{\mathbf{D}}) = 0. \tag{28}$$

The resulting system (see [2]) is

$$\frac{1}{a}\dot{\bar{\mathbf{V}}}' = \mathbf{R}^{\mathrm{T}} \cdot \mathbf{D}' \cdot \mathbf{R} - \bar{\mathbf{D}}', \tag{29}$$

$$\dot{J} = J\mathrm{tr}(\mathbf{D}), \tag{30}$$

$$\begin{aligned}\dot{\mathbf{R}} \cdot \mathbf{R}^{\mathrm{T}} &= \mathbf{W}^{\mathrm{R}} \\ &= \mathbf{W} - \mathbf{R} \cdot \bar{\mathbf{W}} \cdot \mathbf{R}^{\mathrm{T}} \\ &\quad - \frac{1}{a}\mathbf{R} \cdot \left[\bar{\mathbf{V}}' \cdot \left(\bar{\mathbf{D}}' + \frac{1}{2a}\dot{\bar{\mathbf{V}}}'\right) - \left(\bar{\mathbf{D}}' + \frac{1}{2a}\dot{\bar{\mathbf{V}}}'\right) \cdot \bar{\mathbf{V}}'\right] \cdot \mathbf{R}^{\mathrm{T}},\end{aligned} \tag{31}$$

where $\mathbf{A}'$ denotes the deviatoric part of a symmetric second order tensor $\mathbf{A}$. This is a system of nine equations in nine unknowns ($\mathrm{dof}(\bar{\mathbf{V}}') + \mathrm{dof}(J) + \mathrm{dof}(\mathbf{R}) = 5 + 1 + 3$). In addition to clarifying the dynamics described by the kinematic system (*e.g.*, (29) states that the deviatoric stretch component is determined by the difference between the coarse- and fine-scale strain rates), this reformulation also permits an important time scale issue to be addressed in the discrete integration.

Discrete time integration

In high strain rate applications, the right-hand side of (29) will be large, reflecting a fast time-scale relative to that of the coarse-scale model and necessitating an implicit time integration. Given its simple form, equation (30) can be integrated analytically, as can (31) if we lag the evaluation of $\mathbf{W}^{\mathrm{R}}$. Using a backward Euler formula for (29), the system (29)-(31) is integrated from time t_n to time $t_{n+1} = t_n + \Delta t$ via

$$\frac{1}{a_{n+1}\Delta t}\left(\bar{\mathbf{V}}'_{n+1} - \bar{\mathbf{V}}'_{n}\right) = \mathbf{R}^{\mathrm{T}}_{n+1} \cdot \mathbf{D}'_{n+1} \cdot \mathbf{R}_{n+1} - \bar{\mathbf{D}}'_{n+1}, \tag{32}$$

$$J_{n+1} = \exp\left(\mathrm{tr}\left(\mathbf{D}_n\right)\Delta t\right) J_n, \tag{33}$$

$$\mathbf{R}_{n+1} = \exp\left(\mathbf{W}^{\mathrm{R}}_n \Delta t\right) \mathbf{R}_n. \tag{34}$$

Implicit update of the deviatoric stretch tensor

With respect to $\bar{\mathbf{V}}'_{n+1}$, (32) is a nonlinear equation, since, from (26) and (19),

$$\begin{aligned}\bar{\mathbf{D}}'_{n+1} &= \frac{1}{2}\left[\bar{\mathbf{L}}(\bar{\boldsymbol{\tau}}_{n+1}) + \bar{\mathbf{L}}^{\mathrm{T}}(\bar{\boldsymbol{\tau}}_{n+1})\right]' \\ &= \frac{1}{2}\left[\bar{\mathbf{L}}\left(\frac{2G}{a}\bar{\mathbf{V}}'_{n+1}\right) + \bar{\mathbf{L}}^{\mathrm{T}}\left(\frac{2G}{a}\bar{\mathbf{V}}'_{n+1}\right)\right]'.\end{aligned} \tag{35}$$

Writing (32) in the residual form

$$F\left(\bar{\mathbf{V}}'_{n+1}\right) \equiv \frac{1}{a_{n+1}\Delta t}\left(\bar{\mathbf{V}}'_{n+1} - \bar{\mathbf{V}}'_{n}\right) - \mathbf{R}^{\mathrm{T}}_{n+1} \cdot \mathbf{D}'_{n+1} \cdot \mathbf{R}_{n+1} + \bar{\mathbf{D}}'_{n+1} = 0, \tag{36}$$

we apply a Newton procedure to generate a sequence of approximations $\bar{\mathbf{V}}'^{(k)}_{n+1}$, $k = 1, 2, \ldots$, initialized by $\bar{\mathbf{V}}'^{(0)}_{n+1} = \bar{\mathbf{V}}'_n$:

$$\bar{\mathbf{V}}'^{(k+1)}_{n+1} = \bar{\mathbf{V}}'^{(k)}_{n+1} + \delta\bar{\mathbf{V}}'^{(k)}_{n+1} \tag{37}$$

where $\delta\bar{\mathbf{V}}'^{(k)}_{n+1}$ is the solution of

$$\left[\frac{\partial F}{\partial \bar{\mathbf{V}}'}\left(\bar{\mathbf{V}}'^{(k)}_{n+1}\right)\right]\delta\bar{\mathbf{V}}'^{(k)}_{n+1} = -F\left(\bar{\mathbf{V}}'^{(k)}_{n+1}\right), \tag{38}$$

whose coefficient matrix is the Jacobian

$$\begin{aligned}\frac{\partial F}{\partial \bar{\mathbf{V}}'}\left(\bar{\mathbf{V}}'^{(k)}_{n+1}\right) &= \frac{1}{a_{n+1}\Delta t}\mathbf{I} + \frac{2G}{a}\frac{\partial \bar{\mathbf{D}}'_{n+1}}{\partial \bar{\boldsymbol{\tau}}'}\left(\frac{2G}{a}\bar{\mathbf{V}}'^{(k)}_{n+1}\right) \\ &= \frac{1}{a_{n+1}\Delta t}\mathbf{I} + \frac{G}{a}\left[\frac{\partial \bar{\mathbf{L}}}{\partial \bar{\boldsymbol{\tau}}'}\left(\frac{2G}{a}\bar{\mathbf{V}}'^{(k)}_{n+1}\right) + \frac{\partial \bar{\mathbf{L}}^{\mathrm{T}}}{\partial \bar{\boldsymbol{\tau}}'}\left(\frac{2G}{a}\bar{\mathbf{V}}'^{(k)}_{n+1}\right)\right]'.\end{aligned} \tag{39}$$

The evaluation of (36) and (39) therefore requires $\bar{\mathbf{L}}$ and $\partial\bar{\mathbf{L}}/\partial\bar{\boldsymbol{\tau}}'$ evaluated at given values of $\bar{\boldsymbol{\tau}}'$, which is provided by the fine-scale model.

5 Fine-scale viscoplasticity model

CoEVP is designed to enable a fine-scale viscoplasticity model to be incorporated in a modular fashion. A C++ abstract base class defines a generic fine-scale model interface in which the inputs and outputs are passed as Standard Template Library (STL) vectors of doubles. As distributed, CoEVP provides a simple parameterized flow rule as an example concrete derived class. Given $\bar{\boldsymbol{\tau}}'$, the fine-scale strain rate is given by

$$\bar{\mathbf{L}} = \bar{\mathbf{D}} = D_0\frac{\bar{\boldsymbol{\tau}}'}{\parallel \bar{\boldsymbol{\tau}}' \parallel}\left(\frac{\parallel \bar{\boldsymbol{\tau}}' \parallel}{g}\right)^m, \tag{40}$$

where D_0 is a reference strain rate, m is a material sensitivity and g is a hardness parameter. Once constructed with specified D_0, m and g, the fine-scale model object inputs the components of $\bar{\boldsymbol{\tau}}'$ in a vector and returns the components of $\bar{\mathbf{L}}$ in another vector.

6 Specification for the integration of the coupled coarse- and fine-scale systems over a time step

We now describe a step-by-step specification for the integration of the coupled multiscale system from time t_n to time $t_{n+1} = t_n + \Delta t$. We begin by assuming that all quantities are known at time t_n. Subscripts indicate the time at which quantities are evaluated, *e.g.*, $\rho_n \equiv \rho(t_n)$. A schematic diagram of the specification is contained in Figures 1 and 2.

Coarse-scale model update

Procedure C1: Given $\mathbf{x}_n$, $\mathbf{v}_n$, η_n, $\boldsymbol{\sigma}_n$, q_n and $\mathbf{L}_n$, integrate (1)-(7) from time $t = t_n$ to $t = t_{n+1}$, yielding $\mathbf{x}_{n+1}$, $\mathbf{v}_{n+1}$, η_{n+1} and e_{n+1}. Compute $q_{n+1} = q(\mathbf{v}_{n+1})$ and $\mathbf{L}_{n+1}$.

Procedure C2: Compute the new deviatoric stress $\boldsymbol{\sigma}'_{n+1} = \boldsymbol{\sigma}_{n+1} + (p_{n+1} + q(\mathbf{v}_{n+1}))\mathbf{I}$ using the stress $\boldsymbol{\sigma}_{n+1}$ obtained from Procedure K7(c) and pressure p_{n+1} obtained from Procedure K2(c).

Kinematic variable update

Procedure K1: Given $\mathbf{V}_n$, $\dot{\bar{\mathbf{V}}}'_n$, $\mathbf{R}_n$, $\mathbf{L}_n$, $\bar{\mathbf{L}}_n$ and $\mathbf{L}_{n+1}$,

(a) Set $\bar{\mathbf{V}}_n \equiv \mathbf{R}_n^{\mathrm{T}} \cdot \mathbf{V}_n \cdot \mathbf{R}_n$,

(b) Set $J_n \equiv \det(\mathbf{V}_n)$,

(c) Set $a_n \equiv J_n^{1/3}$,

(d) Set $\mathbf{D}_m \equiv \frac{1}{2}\left(\mathbf{L}_m + \mathbf{L}_m^{\mathrm{T}}\right), \quad m = n, n+1$,

(e) Set $\bar{\mathbf{D}}_n \equiv \frac{1}{2}\left(\bar{\mathbf{L}}_n + \bar{\mathbf{L}}_n^{\mathrm{T}}\right)$,

(f) Set $\mathbf{W}_n \equiv \frac{1}{2}\left(\mathbf{L}_n - \mathbf{L}_n^{\mathrm{T}}\right)$,

(g) Set $\bar{\mathbf{W}}_n \equiv \frac{1}{2}\left(\bar{\mathbf{L}}_n - \bar{\mathbf{L}}_n^{\mathrm{T}}\right)$,

(h) Set $\mathbf{W}_n^{\mathrm{R}} \equiv \dot{\mathbf{R}}_n \cdot \mathbf{R}_n^{\mathrm{T}}$
$= \mathbf{W}_n - \mathbf{R}_n \cdot \bar{\mathbf{W}}_n \cdot \mathbf{R}_n^{\mathrm{T}}$
$- \frac{1}{a_n}\mathbf{R}_n \cdot \left[\bar{\mathbf{V}}'_n \cdot \left(\bar{\mathbf{D}}'_n + \frac{1}{2a_n}\bar{\mathbf{V}}'_m\right) - \left(\bar{\mathbf{D}}'_n + \frac{1}{2a_n}\bar{\mathbf{V}}'_m\right) \cdot \bar{\mathbf{V}}'_n\right] \cdot \mathbf{R}_n^{\mathrm{T}}$.

Procedure K2: Integrate the kinematic system:

(a) Set $\mathbf{R}_{n+1} = \exp\left(\mathrm{tr}(\mathbf{W}_n^{\mathrm{R}})\Delta t\right)\mathbf{R}_n$,

(b) Set $J_{n+1} = \exp\left(\mathrm{tr}(\mathbf{D}_n)\Delta t\right) J_n$ and $a_{n+1} = J_{n+1}^{1/3}$,

(c) Compute p_{n+1} using Procedure K3,

(d) Solve

$$F(\bar{\mathbf{V}}'_{n+1}) \equiv \frac{1}{a_{n+1}\Delta t}\left(\bar{\mathbf{V}}'_{n+1} - \bar{\mathbf{V}}'_n\right) + \bar{\mathbf{D}}'_{n+1} - \mathbf{R}_{n+1}^{\mathrm{T}} \cdot \mathbf{D}'_{n+1} \cdot \mathbf{R}_{n+1} = 0 \qquad (41)$$

for $\bar{\mathbf{V}}'_{n+1}$ using Procedure K4.

Procedure K3: Set $p_{n+1} = p(e_{n+1}, J_{n+1})$ using (21).

Procedure K4: Perform a Newton iteration, using Procedure K5 to evaluate the Newton residual (36) and its corresponding Jacobian (39) and Procedure K6 to solve the Jacobian system.

Procedure K5: Given a Newton iterate $\bar{\mathbf{V}}'^{(k)}_{n+1}$, ($k$ is the iteration index),

(a) Set $\bar{\mathbf{E}}'^{(k)}_{n+1} = \frac{1}{a_{n+1}}\bar{\mathbf{V}}'^{(k)}_{n+1}$,

(b) Set $\bar{\boldsymbol{\tau}}'^{(k)} \equiv 2G\bar{\mathbf{E}}'^{(k)}_{n+1}$, where G is a constant shear modulus,

(c) Using $\bar{\boldsymbol{\tau}}'^{(k)}$, get $\bar{\mathbf{L}}$ and $\partial\bar{\mathbf{L}}/\partial\bar{\boldsymbol{\tau}}'$ using Procedure K1,

(d) Set $\bar{\mathbf{D}}^{(k)}_{n+1} \equiv \bar{\mathbf{L}}$,

(e) Evaluate (36) and (39).

Procedure K6: Solve (38).

Procedure K7: Given the solution $\bar{\mathbf{V}}'_{n+1}$ of the Newton solve,

(a) Set $\bar{\boldsymbol{\tau}}_{n+1} = (p_{n+1} + q_{n+1})\mathbf{I} + \frac{2G}{a_{n+1}}\bar{\mathbf{V}}'_{n+1}$,

(b) Set $\bar{\boldsymbol{\sigma}}_{n+1} = J_{n+1}^{-1}\bar{\boldsymbol{\tau}}_{n+1}$,

(c) Set $\boldsymbol{\sigma}_{n+1} = \mathbf{R}_{n+1} \cdot \bar{\boldsymbol{\sigma}}_{n+1} \cdot \mathbf{R}_{n+1}^{\mathrm{T}}$.

Fine-scale model evaluation

Procedure F1: Evaluate $\bar{\mathbf{L}}$ and its $\bar{\boldsymbol{\tau}}$ derivative using adaptive sampling and update the history $\mathcal{H}$, which consists solely of the hardness parameter g.

Procedure F2: Query the interpolation model database for the k^{th} nearest neighbors to $(\bar{\boldsymbol{\tau}}_{n+1}, g)$ based on a prescribed tolerance.

Procedure F3: If the set of nearest neighbor interpolation models is non-empty, use the interpolation models to interpolate $\bar{\mathbf{L}}$ and its derivative at $(\bar{\boldsymbol{\tau}}_{n+1}, g)$. Compute the error estimate.

Procedure F4: If the error tolerance is exceeded, or no interpolation models are close enough, evaluate the fine-scale plasticity model (40) to compute a new $\bar{\mathbf{L}}$ and g. Otherwise, return $\bar{\mathbf{L}}$ and its derivative.

Procedure F5: Add the new fine-scale evaluation to an existing model in the nearest neighbor set. Otherwise, create a new model. Update the database with the new objects created in either case.

Procedure F6: Use the interpolation model to compute the derivative $\partial\bar{\mathbf{L}}/\partial\bar{\boldsymbol{\tau}}$.

7 Adaptive sampling database objects

Evaluation of the stress tensor $\boldsymbol{\sigma}$ at each time step at all of the quadrature points used in the finite element discretization implies a large number of fine-scale model calculations. As described in the fine-scale model evaluation part of the previous section, adaptive sampling attempts to significantly reduce the number of fine-scale evaluations by dynamically constructing a database of interpolation models based on previous fine-scale evaluations. The objects stored in the database used by the database consist not only of fine-scale model evaluations, but also certain interpolation coefficients constructed by the kriging interpolation algorithm. To define these precisely, we summarize the kriging algorithm used in the ASPA proxy app [6].

Summary of univariate kriging algorithm

Kriging is a type of scattered data interpolation first developed in the field of geostatistics. Given a set of experimental measurements, the goal is to estimate the response at points for which no measurements exist. Rather than basing the interpolant simply on some measure of

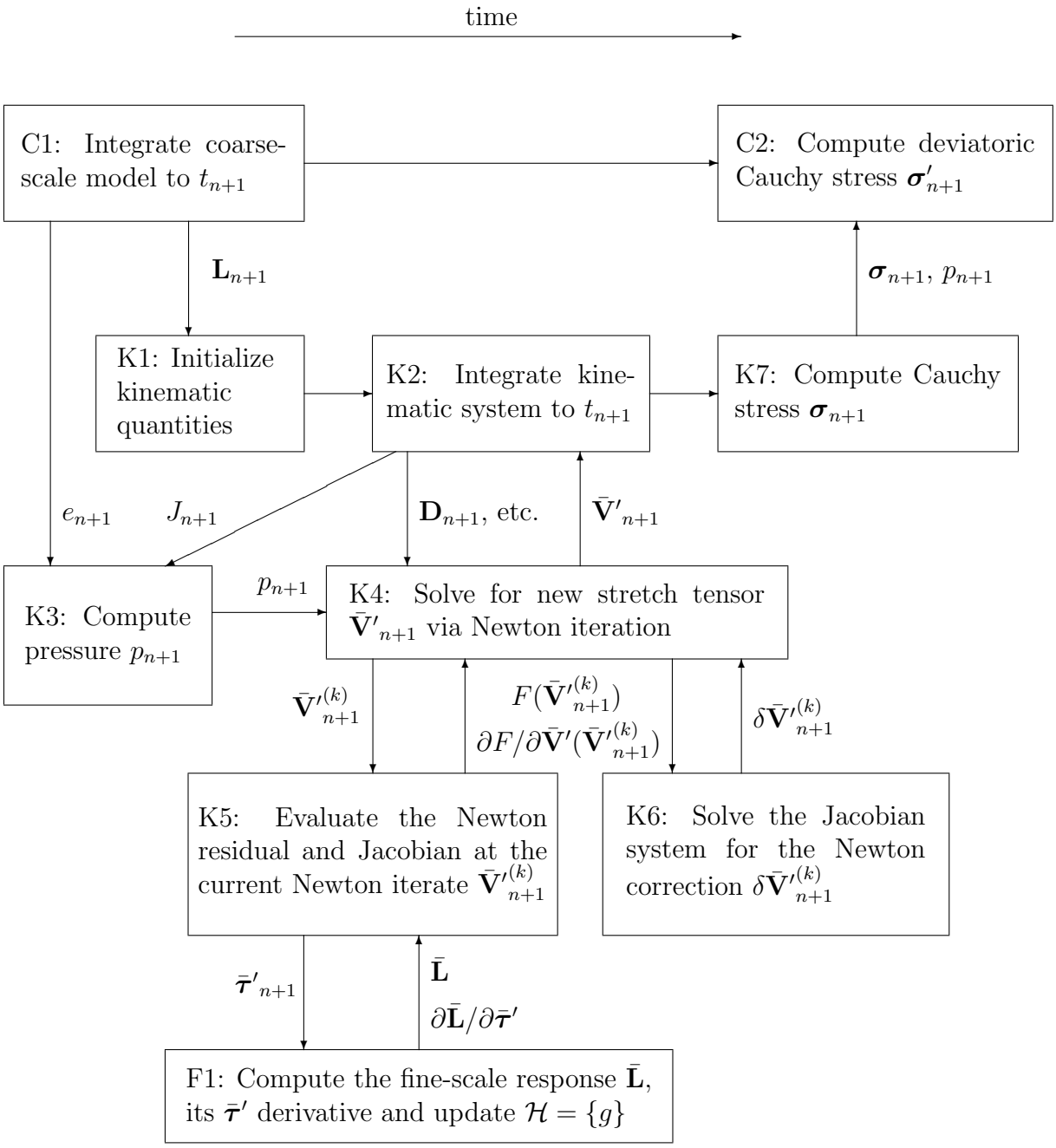

Figure 1: Coupled integration schematic (Part I).

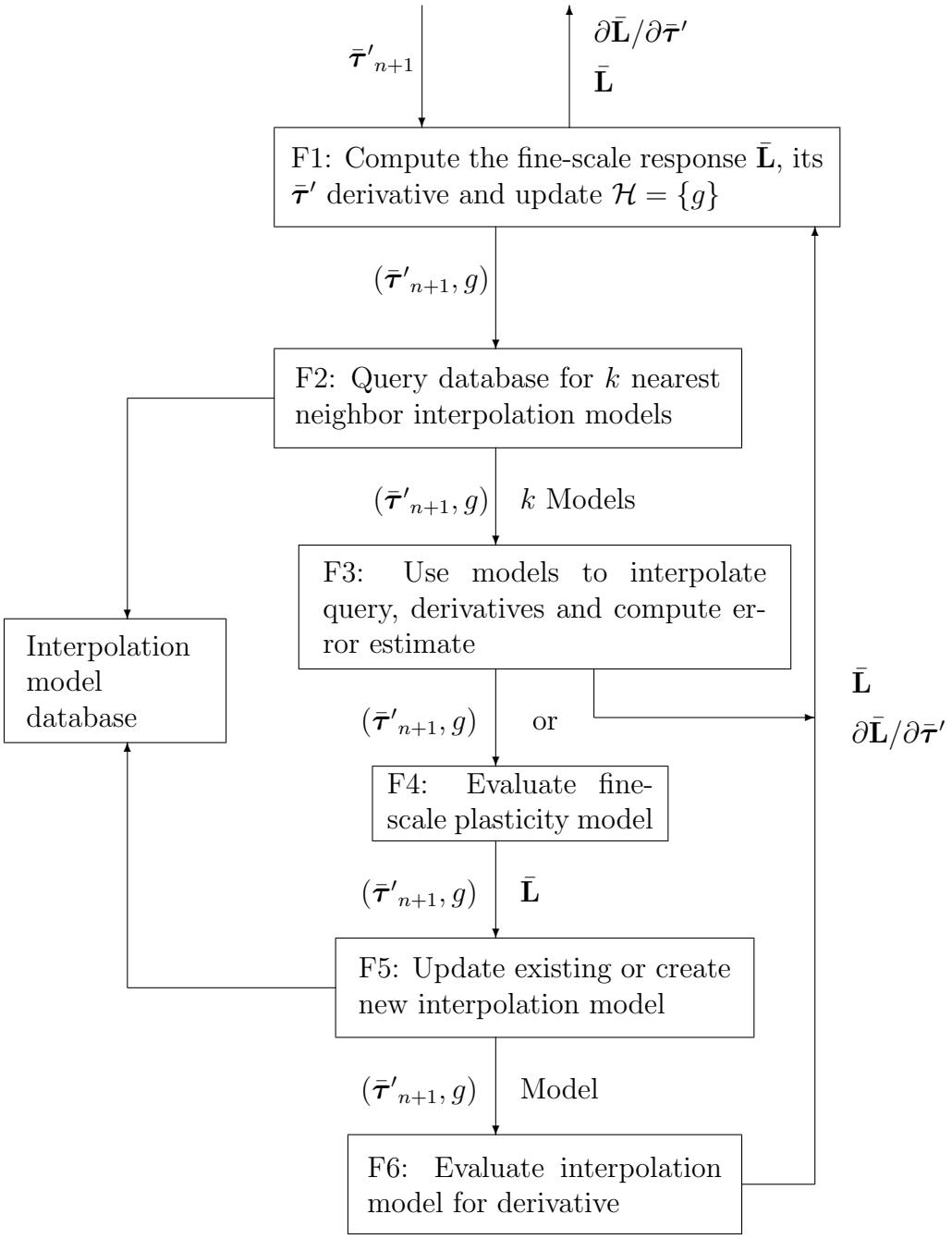

Figure 2: Coupled integration schematic (Part II).

the distance to known points, kriging interpolation attempts to also incorporate information about data correlation. If, for example, a large number of experimental observations exist in a small region, it is possible that the data is sufficiently correlated that much of it is redundant. Depending upon the interpolation goals, failure to account for the correlation of clustered data could potentially result in undesirable over-weighting. The estimation of data correlation is therefore conducted as a precursor to kriging interpolation, involving, for example, the creation of a variogram.

Kriging interpolation assumes that, over some region $\Omega \subset \mathbb{R}^D$, the function being interpolated can be expressed as the sum of a regression (a.k.a. trend) model and a stochastic deviation

$$s(\mathbf{x}) = m(\mathbf{x}) + Z(\mathbf{x}), \tag{42}$$

where $Z(\mathbf{x})$ is assumed to have zero mean and covariance of the form

$$Cov\left\{Z(\mathbf{x}, \mathbf{w})\right\} = \sigma^2 R(\mathbf{x}, \mathbf{w}) \tag{43}$$

with σ^2 denoting the process variance. Typically, a linear regression model

$$m(\mathbf{x}) = \mathbf{p^T}(\mathbf{x})\beta \tag{44}$$

is assumed, where the components of $\mathbf{p}(\mathbf{x}) \equiv [\mathbf{p}_1(\mathbf{x}), \mathbf{p}_2(\mathbf{x}), \ldots, \mathbf{p}_D(\mathbf{x})]$ form a basis for the space of linear mappings of Ω into $\mathbb{R}$ and $\beta \in \mathbb{R}^D$ is a vector of regression coefficients. Given known values of s at points $\mathbf{x}_i \in \Omega$, $i = 1, \ldots, N$, the kriging interpolant is defined as

$$\hat{s}(\mathbf{x}) \equiv m(\mathbf{x}) + \sum_{i=1}^{N} \lambda_i(\mathbf{x})(s(\mathbf{x}_i) - m(\mathbf{x}_i)), \quad \mathbf{x} \in \Omega, \tag{45}$$

where the coefficients $\lambda_i(\mathbf{x})$ are chosen to minimize the error variance

$$\begin{aligned} Var(\hat{s}(\mathbf{x}) - s(\mathbf{x})) &= Var\{\hat{s}(\mathbf{x}) - m(\mathbf{x}) - (s(\mathbf{x}) - m(\mathbf{x}))\} \\ &= Var\left\{\sum_{i=1}^{N} \lambda_i(\mathbf{x})(s(\mathbf{x}_i) - m(\mathbf{x}_i))\right\} + Var\left\{s(\mathbf{x}) - m(\mathbf{x})\right\} \\ &\quad - 2Cov\left\{\sum_{i=1}^{N} \lambda_i(\mathbf{x})(s(\mathbf{x}_i) - m(\mathbf{x}_i)), s(\mathbf{x}) - m(\mathbf{x})\right\} \\ &= \sigma^2 \left(\sum_{i=1}^{N}\sum_{j=1}^{N} \lambda_i(\mathbf{x})\lambda_j(\mathbf{x})R(\mathbf{x}_i, \mathbf{x}_j) + 1 - 2\sum_{i=1}^{N} \lambda_i(\mathbf{x})R(\mathbf{x}_i, \mathbf{x})\right), \end{aligned} \tag{46}$$

subject to the constraint

$$\mathbf{p}(\mathbf{x}) - \sum_{i=1}^{N} \lambda_i(\mathbf{x})\mathbf{p}(\mathbf{x_i}) = 0. \tag{47}$$

The condition (47) ensures that the error expectation $E\{\hat{s}(\mathbf{x}) - s(\mathbf{x})\}$ vanishes independently of the regression coefficients β. By introducing Lagrange multipliers corresponding to (47),

Parameter	Value
k_1	196.8 GPa
k_2	259.8 GPa
k_3	256.6 GPa
Γ	1.60

Table 1: Mie-Gruneisen model parameters for tantalum.

the resulting unconstrained minimization problem is solved by finding the critical point of the augmented system. The result is [3]

$$\lambda(\mathbf{x}) \equiv [\lambda_1(\mathbf{x}), \lambda_2(\mathbf{x}), \ldots, \lambda_N(\mathbf{x})] = \mathbf{r}^{\mathbf{T}}(\mathbf{x})\mathbf{R}^{-1}, \tag{48}$$

$$\beta \equiv [\beta_1, \beta_2, \ldots, \beta_D] = \left(\mathbf{P}^{\mathbf{T}}\mathbf{R}^{-1}\mathbf{P}\right)^{-1}\mathbf{P}^{\mathbf{T}}\mathbf{R}^{-1}\mathbf{v}, \tag{49}$$

where $\mathbf{v} \equiv [s(\mathbf{x}_1), s(\mathbf{x}_2), \ldots, s(\mathbf{x}_N)]$ is the vector of known data,

$$\mathbf{P} \equiv \begin{bmatrix} p_1(\mathbf{x}_1) & \ldots & p_D(\mathbf{x}_1) \\ \ldots & \ddots & \ldots \\ p_1(\mathbf{x}_N) & \ldots & p_D(\mathbf{x}_N) \end{bmatrix}, \tag{50}$$

$$\mathbf{R} \equiv \begin{bmatrix} 1 & R(\mathbf{x}_1, \mathbf{x}_2) & \ldots & R(\mathbf{x}_1, \mathbf{x}_N) \\ R(\mathbf{x}_2, \mathbf{x}_1) & 1 & \ldots & R(\mathbf{x}_2, \mathbf{x}_N) \\ \ldots & \ldots & \ddots & \ldots \\ R(\mathbf{x}_N, \mathbf{x}_1) & \ldots & R(\mathbf{x}_N, \mathbf{x}_{N-1}) & 1 \end{bmatrix}, \tag{51}$$

and

$$\mathbf{r}(\mathbf{x}) \equiv \begin{bmatrix} R(\mathbf{x}_1, \mathbf{x}) \\ \ldots \\ R(\mathbf{x}_N, \mathbf{x}) \end{bmatrix}. \tag{52}$$

8 Example problem

As distributed, CoEVP solves the Taylor cylinder impact problem discussed in [7]. A 30 caliber (7.62 mm diameter) tantalum cylinder of length 38.1 mm is fired at a stationary wall with a normal velocity of 175 m/s. The reference density is 16.64 g/cm^3. The Mie-Gruneisen equation of state (20) is assumed with the parameters given in Table 1. The bulk modulus used in the sound speed estimate (24) is $K = 194$ GPa and the shear modulus used there and in the elasticity model (18)-(19) is $G = 69$ GPa. The flow rule (40) is used as the fine-scale plasticity model, with $D_0 = 10^{-2}\mu$s, $m = 20$ and $g = 0.2$ GPa.

Figure 3 shows the cylinder deformation after 0.1 μs colored by the computed energy. Only the half of the cylinder nearest the wall is shown.

References

[1] `www.exmatex.org`.

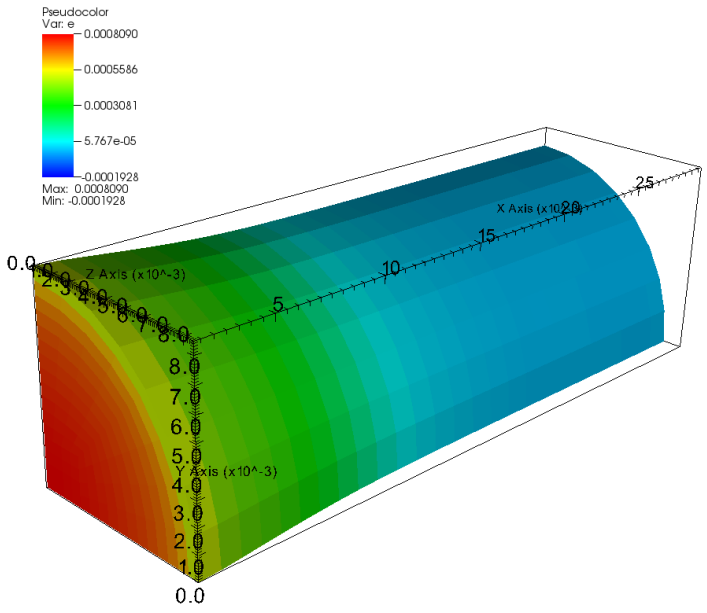

Figure 3: Energy plot at 0.1 μs for Taylor cylinder test.

[2] N. R. Barton, J. Knap, A. Arsenlis, R. Becker, R. D. Hornung and D. R. Jefferson, "Embedded Polycrystal Plasticity and Adaptive Sampling," International Journal of Plasticity 24 (2008), pp. 242–266.

[3] J. Knap, N. R. Barton, R. D. Hornung, A. Arsenlis, R. Becker and D. R. Jefferson, "Adaptive Sampling in Hierarchical Simulation," International Journal for Numerical Methods in Engineering 76 (2008), pp. 572–600.

[4] `wci.llnl.gov/codes/ale3d/index.html`.

[5] `codesign.llnl.gov/lulesh.php`.

[6] `www.exmatex.org/aspa.html`.

[7] P. J. Maudlin, J. F. Bingert, J. W. House and S. R. Chen, "On the Modeling of the Taylor Cylinder Impact Test for Orthotropic Textured Materials: Experiments and Simulations," Inter. J. Plasticity 15 (1999), pp. 139-166,

[8] Nathan Barton, "Cold energy integration", Lawrence Livermore National Laboratory technical report, UCRL-TR-220933.

[9] R. B. Christensen, "Godunov Methods on a Staggered Mesh, An Improved Artificial Viscosity", Lawrence Livermore National Laboratory Report UCRL-JC-105269.